Acta Mech 227, 1621–1643 (2016)
DOI 10.1007/s00707-016-1570-0

ORIGINAL PAPER

M. Hosseini · M. Bahreman · A. Jamalpoor

# Using the modified strain gradient theory to investigate the size-dependent biaxial buckling analysis of an orthotropic multi-microplate system

Received: 15 October 2015 / Revised: 6 December 2015 / Published online: 23 February 2016


**Abstract** On the basis of the modified strain gradient theory, this research presents an analytical approach to analyze elastic instability of an orthotropic multi-microplate system (OMMPS) embedded in a Pasternak elastic medium under biaxial compressive loads. Kirchhoff plate theory and the principle of total potential energy are applied to obtain the partial differential equations and corresponding boundary conditions. Various types of "chain" boundary conditions for the ends of the microplates system are assumed such as "Clamped-Chain," "Free-Chain" and "Cantilever-Chain" systems. In order to analytically obtain the buckling load of the OMMPS, we use Navier's approach which satisfies the simply supported boundary conditions and trigonometric method. In order to show the dependability of the presented formulation in this paper, several comparison studies are carried out to compare with existing data in the literature. Numerical results are presented to reveal variations of the buckling load of OMMPS corresponding to various values of the number of microplates, the length scale parameter $\left(\frac{h}{l}\right)$, aspect ratio, Pasternak elastic medium parameters and the thickness of the microplate and the biaxial compression ratio. Some numerical results of this paper illustrate that when the number of microplates is small, especially becoming 2, there is an important difference between buckling loads obtained for "Clamped-Chain," "Free-Chain" and "Cantilever-Chain" systems. Also, it is shown that by increasing the number of microplates in the system, the influence of the Pasternak elastic medium on the buckling load of system is reduced. It is anticipated that the results reported in this work are applied as a benchmark in future microstructure issues.

## 1 Introduction

Over the last years, micro- and nanoscale structures have been vastly applied in different engineering fields due to their superior properties. Size-dependent effects are significant in micro- and nanoscale structures. Classical theories do not include size effects and have inaccurate results for micro-/nanoscales [1–3]. Various non-classical continuum approaches such as couple stress theory [4–6], strain gradient theory [7,8], non-local elasticity theory [9,10] and micropolar theory [11] have been proposed in the literature. These theories were

M. Hosseini (✉)
Department of Mechanical Engineering, Sirjan University of Technology, Sirjan 78137-33385, Islamic Republic of Iran
E-mail: hosseini@sirjantech.ac.ir
Tel.: +98 34 42 33 69 01
Fax: +98 34 42 33 69 00

M. Bahreman
Department of Mechanical Engineering, Shahid Bahonar University of Kerman, Kerman, Islamic Republic of Iran

A. Jamalpoor
Department of Mechanical Engineering, Iran University of Science and Technology, Narmak,
Tehran 16846-13114, Islamic Republic of Iran

developed based on the supposed constitutive law and strain energy of the structures and consider the effects of small scales for micro-/nanoscale structures. Many types of research have been accomplished in recent years to investigate the bending, buckling and free vibration behavior of these structures based on the mentioned theories.

Non-local elasticity theory is a well-known theory that accounts for the scale effect. In this theory, it is assumed that the stress at a reference point depends on the strains at all the points in the body. Many types of research have been done to analyze nanoscale structures on the basis of non-local elasticity theory including vibration [12–14], buckling [15,16] and bending [17].

Strain gradient theory (SGT) is one of the continuum approaches with five material length scale parameters corresponding to the second-order gradient of deformations developed by Fleck and Hutchinson [8]. After that, Lam et al. [18] modified and improved the strain gradient theory by decomposing the second-order deformation gradients into three parts and assigning three length scales to each part. Based on the modified strain gradient theory (MSGT), Kong et al. [19], Akgöz and Civalek [20] and Asghari et al. [21] carried out static and dynamic analysis of microbeams on the basis of Bernoulli–Euler and Timoshenko beam models. Ansari et al. [22] investigated the free vibration analysis of size-dependent functionally graded microbeams based on the strain gradient Timoshenko beam theory. A solution for bending analysis of a rectangular microscale Kirchhoff plate using MSGT was provided by Movassagh and Mahmoodi [23]. Jamalpoor and Hosseini [24] carried out biaxial buckling analysis of double-orthotropic microplate systems including in-plane magnetic field based on MSGT.

The modified couple stress theory (MCST) involving only one material length scale parameter was elaborated by [25]. This theory is derived from the classical couple stress theory and includes asymmetric couple stress tensor. Using MCST, multiple size-dependent beam and plate models have been reported to consider the size effects in micro- and nanoscale structures. An Euler–Bernoulli beam model for bending analysis of nanobeams was proposed by Park and Gao [26]. On the basis of the MCST and Kirchhoff plate approach, Tsiatas and Yiotis [27] proposed a new model to investigate the static, dynamic and buckling behavior of an orthotropic skew microplate. Recently, Şimşek et al. [28] employed MCST in conjunction with Kirchhoff plate theory to study the dynamic response of a rectangular microplate due to a moving force. Ma et al. [29] proposed a Timoshenko beam model to accommodate the effects of transverse shear deformation and rotary inertia. This model was used to study the buckling of microtubules (Fu and Zhang [30]) and vibration of nanotubes (Ke and Wang [31]). Yin et al. [32] studied the vibration of microplates based on MCST. Ma et al. [33] and Ke et al. [34] proposed a Mindlin plate model to take into account the effects of transverse shear deformation and rotary inertia in moderately thick microplates. In another study, Lou and He [35] extracted closed-form solutions for nonlinear bending and free vibration of functionally graded microplates using MCST and the Kirchhoff/Mindlin plate theory.

However, by review of papers reporting buckling analysis of microplates according to MSGT, it is found that no study has been presented in the literature on biaxial buckling analysis of orthotropic multi-microplate system (OMMPS) embedded in a Pasternak elastic medium. The present study focuses on modeling the buckling behavior of a size-dependent OMMPS in a Pasternak elastic foundation. Also in this paper, a kind of the analytical method (so-called trigonometric method) is used for the buckling analysis of a multi-microplate system. Simply supported boundary conditions are assumed for all edges of the microplates for three different "chain" conditions, "Clamped-Chain," "Free-Chain" and "Cantilever-Chain." Analogical results are presented in tabular form to show the differences between the results obtained from exact and numerical solutions for different "chain" conditions. Furthermore, the effects of various parameters including the additional length scale parameter, higher modes, aspect ratio, Pasternak medium parameters and length scale parameter on the buckling load are studied in detail.

## 2 Modeling of the problem and formulation

### 2.1 Geometrical configuration

Consider a set of orthotropic multiple simply supported rectangular microplates embedded within a Pasternak elastic medium represented by Winkler and shear layers with stiffness coefficients $k$ and $k_1$, respectively, as shown in Fig. 1a. It is assumed that the geometrical and physical characteristics including the uniform thickness of $h$, the length of $L_x$, width of $L_y$, Poisson's ratios of $\vartheta_{12}$ and $\vartheta_{21}$ and Young's modulus in the $x-y$ plane ($E_1$ and $E_2$) are identical for each microplate. Also, the transverse displacements of $Q$-coupled orthotropic

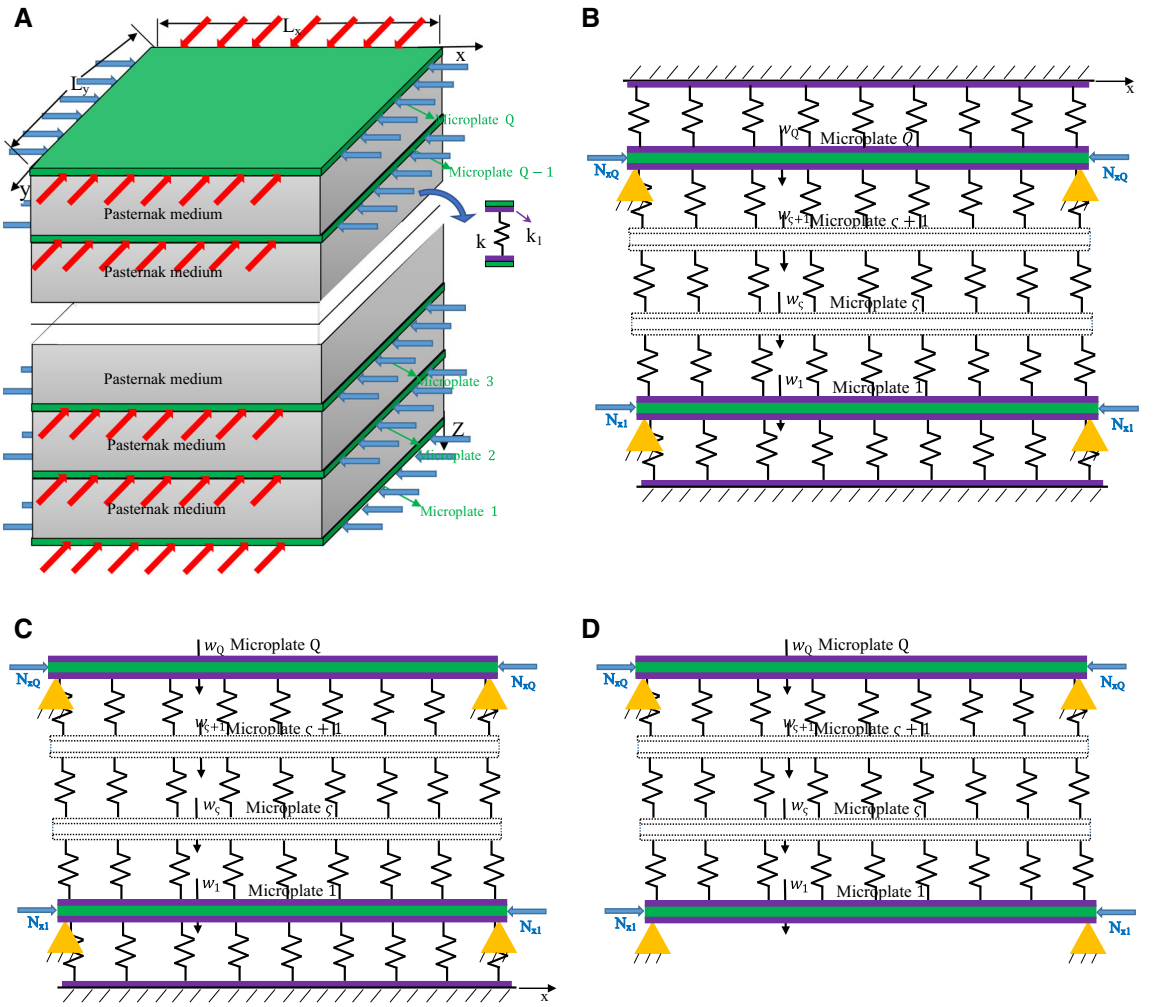


**Fig. 1** Orthotropic multi-microplate system (OMMPS): **a** the geometry of the OMMPS embedded in a Pasternak elastic medium, **b** "Clamped-Chain," **c** "Cantilever-Chain," **d** "Free-Chain"

microplates are displayed by $w_\varsigma\,(x,y)\,,\varsigma=1,2,\ldots,\,Q$. In this study, there is an influence of the size on the elastic instability behavior of multi-microplates for three various types of "chain" boundary conditions such as "Clamped-Chain" (in this case the first and last microplates in the multi-microplate system are linked with a fixed surface by a Pasternak elastic medium, see Fig. 1b), "Cantilever-Chain" (in this case the bottom microplate in the multi-microplate system is linked to the fixed surface by a Pasternak elastic medium, and the top microplate is free, see Fig. 1c) and finally "Free-Chain" (as can be seen in Fig. 1d, the first and last microplates are not linked with the fixed surface).

## 2.2 Formulations

The displacement field $(u_{\varsigma x}, u_{\varsigma y}, u_{\varsigma z})$ of the plate for an arbitrary point of the $\varsigma$-th plate based on the classic (Kirchhoff) plate assumption in Cartesian coordinates is given as follows:

$$u_{\varsigma x}\,(x,y,z)=-z\frac{\partial w_\varsigma}{\partial x},\quad u_{\varsigma y}\,(x,y,z)=-z\frac{\partial w_\varsigma}{\partial y},\quad u_{\varsigma z}\,(x,y,z)=w_\varsigma\,(x,y)\,, \tag{1}$$

where $w_\varsigma$ is the mid-plane transverse deflection of the microplate in the $z$ direction. Also, the general strain displacement relations $\varepsilon=[\varepsilon_{xx}\varepsilon_{yy}\varepsilon_{xy}]^T$ in terms of the deflections are expressed as

$$\varepsilon_{xx} = -z\frac{\partial^2 w_\varsigma}{\partial x^2}, \quad \varepsilon_{yy} = -z\frac{\partial^2 w_\varsigma}{\partial y^2}, \quad \gamma_{xy} = -2z\frac{\partial^2 w_\varsigma}{\partial x \partial y}, \tag{2}$$

where $\varepsilon_{xx}$ and $\varepsilon_{yy}$ are the normal strain components and $\gamma_{xy}$ is the shear strain component. The classical stress–strain relation for an orthotropic microplate for two-dimensional elasticity can be obtained as

$$\begin{bmatrix} \sigma_{xx} \\ \sigma_{yy} \\ \sigma_{xy} \end{bmatrix} = \begin{bmatrix} \frac{E_1}{1-\vartheta_{12}\vartheta_{21}} & \frac{\vartheta_{12}E_2}{1-\vartheta_{12}\vartheta_{21}} & 0 \\ \frac{\vartheta_{12}E_2}{1-\vartheta_{12}\vartheta_{21}} & \frac{E_2}{1-\vartheta_{12}\vartheta_{21}} & 0 \\ 0 & 0 & \frac{E_1}{2(1+\vartheta_{12})} \end{bmatrix} \begin{bmatrix} \varepsilon_{xx} \\ \varepsilon_{yy} \\ \gamma_{xy} \end{bmatrix}. \tag{3}$$

In order to obtain the governing equilibrium equations and corresponding boundary conditions along the borders $x$ and $y$, the principle of total potential energy is used as

$$\Pi = U + U_b - V, \tag{4}$$

where $U, U_b$ and $V$ denote the stored strain gradient energy of the microplate, the potential energy due to the in-plane pre-buckling loads and the external work exerted by transverse load $q(x, y)$ due to the Pasternak elastic medium, respectively.

### *2.2.1 Strain gradient approach*

It should be noted that to capture the size effect on the buckling behavior of the plate, three independent higher-order internal length scale parameters $(l_0, l_1, l_2)$ should be considered based on the MSGT. MSGT expresses that the total strain energy density of the microplate in addition to the dependence on the classical strain tensor $\varepsilon_{ij}$ is dependent on the dilatation gradient vector $\gamma_i$, the deviatoric stretch gradient tensor $\eta_{ijk}$ and the symmetric rotation gradient tensor $\chi_{ij}$, which can be written as

$$U = \frac{1}{2}\int \left(\sigma_{ij}\varepsilon_{ij} + p_i\gamma_i + \tau_{ijk}\psi_{ijk} + m_{ij}\chi_{ij}\right) dv, \tag{5}$$

in which $p_i$, $\tau_{ijk}$ and $m_{ij}$ display the higher-order stress tensors, which are given by

$$\sigma_{ij} = \lambda\varepsilon_{kk}\delta_{ij} + 2\mu\varepsilon_{ij}, \tag{6a}$$
$$p_i = 2\mu l_0^2\gamma_i, \tag{6b}$$
$$\tau_{ijk} = 2\mu l_1^2\psi_{ijk}, \tag{6c}$$
$$m_{ij} = 2\mu l_2^2\chi_{ij}, \tag{6d}$$

where $\lambda$ and $\mu$ are the Lamé constants. Also, $\gamma_i$, $\psi_{ijk}$ and $\chi_{ij}$ are given as

$$\gamma_i = \varepsilon_{mm,i}, \tag{7a}$$
$$\psi_{ijk} = \frac{1}{3}\left(\varepsilon_{jk,i}+\varepsilon_{ki,j}+\varepsilon_{ij,k}\right) - \frac{1}{15}\left(\delta_{ij}\left(\varepsilon_{mm,k}+2\varepsilon_{mk,m}\right) + \delta_{jk}\left(\varepsilon_{mm,i}+2\varepsilon_{mi,m}\right) + \delta_{ki}\left(\varepsilon_{mm,j}+2\varepsilon_{mj,m}\right)\right), \tag{7b}$$
$$\chi_{ij} = \frac{1}{4}\left(e_{ipq}\varepsilon_{qj,p} + e_{jpq}\varepsilon_{qi,p}\right), \tag{7c}$$

where $\delta_{ij}$ and $e_{ijk}$ are the Kronecker delta and permutation symbol, respectively. Also, $(,i)$ expresses $\frac{\partial}{\partial i}$. By inserting Eqs. (1) and (2) into Eq. (7), the nonzero constituents of dilatation gradient vector $\gamma_i$, the deviatoric stretch gradient tensor $\psi_{ijk}$ and the symmetric rotation gradient tensor $\chi_{ij}$ can be obtained as

$$\gamma_x = -z\left(\frac{\partial^3 w_\varsigma}{\partial x^3} + \frac{\partial^3 w_\varsigma}{\partial x \partial y^2}\right), \tag{8a}$$
$$\gamma_y = -z\left(\frac{\partial^3 w_\varsigma}{\partial y^3} + \frac{\partial^3 w_\varsigma}{\partial x^2 \partial y}\right), \tag{8b}$$

$$\gamma_z = -\left(\frac{\partial^2 w_\varsigma}{\partial x^2} + \frac{\partial^2 w_\varsigma}{\partial y^2}\right), \tag{8c}$$

$$\psi_{xxx} = \frac{1}{5}z\left(-2\frac{\partial^3 w_\varsigma}{\partial x^3} + 3\frac{\partial^3 w_\varsigma}{\partial x \partial y^2}\right), \tag{8d}$$

$$\psi_{yyy} = \frac{1}{5}z\left(-2\frac{\partial^3 w_\varsigma}{\partial y^3} + 3\frac{\partial^3 w_\varsigma}{\partial x^2 \partial y}\right), \tag{8e}$$

$$\psi_{zzz} = \frac{1}{5}\left(\frac{\partial^2 w_\varsigma}{\partial x^2} + \frac{\partial^2 w_\varsigma}{\partial y^2}\right), \tag{8f}$$

$$\psi_{xxz} = \psi_{xzx} = \psi_{zxx} = \frac{1}{15}\left(-4\frac{\partial^2 w_\varsigma}{\partial x^2} + \frac{\partial^2 w_\varsigma}{\partial y^2}\right), \tag{8g}$$

$$\psi_{yyz} = \psi_{yzy} = \psi_{zyy} = \frac{1}{15}\left(-4\frac{\partial^2 w_\varsigma}{\partial y^2} + \frac{\partial^2 w_\varsigma}{\partial x^2}\right), \tag{8h}$$

$$\psi_{xyy} = \psi_{yxy} = \psi_{yyx} = \frac{1}{5}z\left(-4\frac{\partial^3 w_\varsigma}{\partial x \partial y^2} + \frac{\partial^3 w_\varsigma}{\partial x^3}\right), \tag{8i}$$

$$\psi_{xxy} = \psi_{xyx} = \psi_{yxx} = \frac{1}{5}z\left(-4\frac{\partial^3 w_\varsigma}{\partial x^2 \partial y} + \frac{\partial^3 w_\varsigma}{\partial y^3}\right), \tag{8j}$$

$$\psi_{zxz} = \psi_{zzx} = \psi_{xzz} = \frac{1}{5}z\left(\frac{\partial^3 w_\varsigma}{\partial x \partial y^2} + \frac{\partial^3 w_\varsigma}{\partial x^3}\right), \tag{8k}$$

$$\psi_{zzy} = \psi_{zyz} = \psi_{yzz} = \frac{1}{5}z\left(\frac{\partial^3 w_\varsigma}{\partial x^2 \partial y} + \frac{\partial^3 w_\varsigma}{\partial y^3}\right), \tag{8l}$$

$$\psi_{xyz} = \psi_{yxz} = \psi_{yzx} = \psi_{zxy} = \psi_{zyx} = \psi_{xzy} = -\frac{1}{3}\frac{\partial^2 w_\varsigma}{\partial x \partial y}, \tag{8m}$$

$$\chi_{xx} = \frac{\partial^2 w_\varsigma}{\partial x \partial y}, \tag{8n}$$

$$\chi_{yy} = -\frac{\partial^2 w_\varsigma}{\partial x \partial y}, \tag{8o}$$

$$\chi_{xy} = \frac{1}{2}\left(\frac{\partial^2 w_\varsigma}{\partial y^2} - \frac{\partial^2 w_\varsigma}{\partial x^2}\right). \tag{8p}$$

Finally, the variational form of total stored strain gradient energy of the microplate is given as

$$\begin{aligned}\delta U = \int\int_{-\frac{h}{2}}^{\frac{h}{2}} (&\sigma_{xx}\delta\varepsilon_{xx} + \sigma_{yy}\delta\varepsilon_{yy} + 2\sigma_{xy}\delta\varepsilon_{xy} + p_x\delta\gamma_x + p_y\delta\gamma_y + p_z\delta\gamma_z \\ &+ \tau_{xxx}\delta\psi_{xxx} + 3\tau_{xxy}\delta\psi_{xxy} + 3\tau_{xxz}\delta\psi_{xxz} + 3\tau_{xyy}\delta\psi_{xyy} + \tau_{yyy}\delta\psi_{yyy} \\ &+ 3\tau_{yyz}\delta\psi_{yyz} + 3\tau_{xzz}\delta\psi_{xzz} + 3\tau_{yzz}\delta\psi_{yzz} + \tau_{zzz}\delta\psi_{zzz} + 6\tau_{xyz}\delta\psi_{xyz} \\ &+ m_{xx}\delta\chi_{xx} + m_{yy}\delta\chi_{yy} + 2m_{xy}\delta\chi_{xy})\mathrm{dzdA}.\end{aligned} \tag{9}$$

*2.2.2 Variation of potential energy due to the pre-buckling forces*

The variation of the potential energy under in-plane compressive forces $N_x^0$ and $N_y^0$ and shear force $N_{xy}^0$ is defined as

$$\delta U_b = -\int\left(\left(N_x^0\right)\frac{\partial^2 w_\varsigma}{\partial x^2} + 2N_{xy}^0\frac{\partial^2 w_\varsigma}{\partial x \partial y} + \left(N_y^0\right)\frac{\partial^2 w_\varsigma}{\partial y^2}\right)\delta w_\varsigma \mathrm{dA}. \tag{10}$$

*2.2.3 Variation of work exerted by external forces*

The variation of the external work can be expressed as

$$\delta V = \int \left(q\delta w_\varsigma\right) \mathrm{dA}, \tag{11}$$

where $q$ displays the total reaction pressure exerted on each orthotropic microplate by the Pasternak elastic foundation, which is given as

$$\begin{aligned} q = {} & k\left(w_\varsigma - w_{\varsigma-1}\right) - k\left(w_{\varsigma+1} - w_\varsigma\right) - k_1\left(\frac{\partial^2 w_\varsigma}{\partial x^2} - \frac{\partial^2 w_{\varsigma-1}}{\partial x^2}\right) - k_1\left(\frac{\partial^2 w_\varsigma}{\partial y^2} - \frac{\partial^2 w_{\varsigma-1}}{\partial y^2}\right) \\ & + k_1\left(\frac{\partial^2 w_{\varsigma+1}}{\partial x^2} - \frac{\partial^2 w_\varsigma}{\partial x^2}\right) + k_1\left(\frac{\partial^2 w_{\varsigma+1}}{\partial y^2} - \frac{\partial^2 w_\varsigma}{\partial y^2}\right). \end{aligned} \tag{12}$$

On the basis of the principle of minimum potential energy $\delta\Pi = 0$, the following equilibrium equation for the $\varsigma$-th orthotropic microplate is achieved:

$$\begin{aligned} & \frac{\partial^2 M_{xx}}{\partial x^2} + 2\frac{\partial^2 M_{xy}}{\partial x \partial y} + \frac{\partial^2 M_{yy}}{\partial y^2} - \frac{\partial^3 \Lambda_{xxx}}{\partial x^3} - \frac{\partial^3 \Lambda_{xxy}}{\partial x^2 \partial y} - \frac{\partial^3 \Lambda_{xyy}}{\partial x \partial y^2} \\ & - \frac{\partial^3 \Lambda_{yyy}}{\partial y^3} - N_x^0 \frac{\partial^2 w_\varsigma}{\partial x^2} - N_y^0 \frac{\partial^2 w_\varsigma}{\partial y^2} - 2N_{xy}^0 \frac{\partial^2 w_\varsigma}{\partial x \partial y} + q = 0, \end{aligned} \tag{13}$$

where the new parameters $M_{xx}$, $M_{yy}$, $M_{xy}$, $\Lambda_{xxx}$, $\Lambda_{xxy}$, $\Lambda_{xyy}$ and $\Lambda_{yyy}$ are expressed by the following integral expressions:

$$M_{xx} = \int_{-\frac{h}{2}}^{\frac{h}{2}} \left(\sigma_{xx} z + p_z + \frac{4}{5}\tau_{xxz} - \frac{1}{5}\tau_{yyz} - \frac{1}{5}\tau_{zzz} + m_{xy}\right) dz, \tag{14a}$$

$$M_{xy} = \int_{-\frac{h}{2}}^{\frac{h}{2}} \left(\sigma_{xy} z + \tau_{xyz} - \frac{1}{2}m_{xx} + \frac{1}{2}m_{yy}\right) dz, \tag{14b}$$

$$M_{yy} = \int_{-\frac{h}{2}}^{\frac{h}{2}} \left(\sigma_{yy} z + p_z - \frac{1}{5}\tau_{xxz} + \frac{4}{5}\tau_{yyz} - \frac{1}{5}\tau_{zzz} - m_{xy}\right) dz, \tag{14c}$$

$$\Lambda_{xxx} = \int_{-\frac{h}{2}}^{\frac{h}{2}} \left(p_x + \frac{2}{5}\tau_{xxx} - \frac{3}{5}\tau_{xyy} - \frac{3}{5}\tau_{xzz}\right) z dz, \tag{14d}$$

$$\Lambda_{xxy} = \int_{-\frac{h}{2}}^{\frac{h}{2}} \left(p_y + \frac{12}{5}\tau_{xxy} - \frac{3}{5}\tau_{yyy} - \frac{3}{5}\tau_{yzz}\right) z dz, \tag{14e}$$

$$\Lambda_{xyy} = \int_{-\frac{h}{2}}^{\frac{h}{2}} \left(p_x + \frac{12}{5}\tau_{xyy} - \frac{3}{5}\tau_{xxx} - \frac{3}{5}\tau_{xzz}\right) z dz, \tag{14f}$$

$$\Lambda_{yyy} = \int_{-\frac{h}{2}}^{\frac{h}{2}} \left(p_y + \frac{2}{5}\tau_{yyy} - \frac{3}{5}\tau_{xxy} - \frac{3}{5}\tau_{yzz}\right) z dz. \tag{14g}$$

The above integral expressions can be expressed in terms of deflection by applying Eqs. (3), (6) and (8), which are provided in the Appendix

Also, the boundary condition along the borders $x$ and $y$ with normal vectors $n_x$ and $n_y$ for the $\varsigma$-th orthotropic microplate is written as

$$\begin{aligned} w_\varsigma = 0 \text{ or } n_x & \left(\frac{\partial M_{xx}}{\partial x} + \frac{\partial M_{xy}}{\partial y} - \frac{\partial^2 \Lambda_{xxx}}{\partial x^2} - \frac{1}{2}\frac{\partial^2 \Lambda_{xxy}}{\partial x \partial y} - \frac{1}{2}\frac{\partial^2 \Lambda_{xyy}}{\partial y^2} + k_1\left(\frac{\partial w_\varsigma}{\partial x} - \frac{\partial w_{\varsigma-1}}{\partial x}\right)\right. \\ & \left. - k_1\left(\frac{\partial w_{\varsigma+1}}{\partial x} - \frac{\partial w_\varsigma}{\partial x}\right)\right) + n_y\left(\frac{\partial M_{yy}}{\partial y} + \frac{\partial M_{xy}}{\partial x} - \frac{1}{2}\frac{\partial^2 \Lambda_{xxy}}{\partial x^2} - \frac{1}{2}\frac{\partial^2 \Lambda_{xyy}}{\partial x \partial y} - \frac{\partial^2 \Lambda_{yyy}}{\partial y^2}\right) \end{aligned}$$

$$+k_1\left(\frac{\partial w_\varsigma}{\partial y}-\frac{\partial w_{\varsigma-1}}{\partial y}\right)-k_1\left(\frac{\partial w_{\varsigma+1}}{\partial y}-\frac{\partial w_\varsigma}{\partial y}\right)\Bigg)=0, \tag{15a}$$

$$\frac{\partial w_\varsigma}{\partial x}=0, n_x\left(-M_{xx}+\frac{\partial \Lambda_{xxx}}{\partial x}+\frac{1}{2}\frac{\partial \Lambda_{xxy}}{\partial y}\right)+n_y\left(-M_{xy}+\frac{1}{2}\frac{\partial \Lambda_{xxy}}{\partial x}+\frac{1}{2}\frac{\partial \Lambda_{yyy}}{\partial y}\right)=0, \tag{15b}$$

$$\frac{\partial w_\varsigma}{\partial y}=0, n_x\left(-M_{xy}+\frac{1}{2}\frac{\partial \Lambda_{xxy}}{\partial x}+\frac{1}{2}\frac{\partial \Lambda_{xyy}}{\partial y}\right)+n_y\left(-M_{yy}+\frac{1}{2}\frac{\partial \Lambda_{xyy}}{\partial x}+\frac{1}{2}\frac{\partial \Lambda_{yyy}}{\partial y}\right)=0, \tag{15c}$$

$$\frac{\partial^2 w_\varsigma}{\partial x^2}=0, n_x\Lambda_{xxx}+\frac{1}{2}n_y\Lambda_{xxy}=0, \tag{15d}$$

$$\frac{\partial^2 w_\varsigma}{\partial y^2}=0, \frac{1}{2}\left(n_x\Lambda_{xyy}+n_y\Lambda_{yyy}\right)=0. \tag{15e}$$

In order to simplify, we assume $N_{xy}^0=0$, $\lambda=\frac{N_y^0}{N_x^0}$, and by substituting the relationships (12) and (14) into Eq. (13) in conjunction with Eqs. (2, 6, 8), an explicit term of the governing equation for the $\varsigma$-th orthotropic microplate in terms of transverse deflections can be obtained as follows:

$$\begin{aligned}
&\left(D_{11}+\frac{E_1 h}{2\left(1+\vartheta_{12}\right)}\left(2{l_0}^2+\frac{8}{15}{l_1}^2+{l_2}^2\right)\right)\frac{\partial^4 w_\varsigma}{\partial x^4}\\
&+\left(2\left(D_{12}+2D_{66}\right)+\frac{E_1 h}{2\left(1+\vartheta_{12}\right)}\left(2{l_0}^2+\frac{8}{15}{l_1}^2+{l_2}^2\right)\right)\frac{\partial^4 w_\varsigma}{\partial x^2\partial y^2}\\
&+\left(D_{22}+\frac{E_1 h}{2\left(1+\vartheta_{12}\right)}\left(2{l_0}^2+\frac{8}{15}{l_1}^2+{l_2}^2\right)\right)\frac{\partial^4 w_\varsigma}{\partial y^4}\\
&-\frac{E_1 h^3}{2\left(1+\vartheta_{12}\right)}\left(\frac{{l_0}^2}{6}+\frac{{l_1}^2}{15}\right)\left(\frac{\partial^2 w_\varsigma}{\partial x^2}+\frac{\partial^2 w_\varsigma}{\partial y^2}\right)^3-N_x^0\left(\frac{\partial^2 w_\varsigma}{\partial x^2}+\lambda\frac{\partial^2 w_\varsigma}{\partial y^2}\right)-kw_{\varsigma-1}+2kw_\varsigma-kw_{\varsigma+1}\\
&+k_1\left(\frac{\partial^2 w_{\varsigma-1}}{\partial x^2}+\frac{\partial^2 w_{\varsigma-1}}{\partial y^2}\right)-2k_1\left(\frac{\partial^2 w_\varsigma}{\partial x^2}+\frac{\partial^2 w_\varsigma}{\partial y^2}\right)+k_1\left(\frac{\partial^2 w_{\varsigma+1}}{\partial x^2}+\frac{\partial^2 w_{\varsigma+1}}{\partial y^2}\right)=0.
\end{aligned} \tag{16}$$

Also $D_{11}$, $D_{12}$, $D_{66}$ and $D_{22}$ are the in-plane bending stiffnesses of the orthotropic microplate, which can be expressed as $(D_{11}, D_{12}, D_{66}, D_{22})=\int_{-\frac{h}{2}}^{\frac{h}{2}}\left(\frac{E_1}{(1-\vartheta_{12}\vartheta_{21})}, \frac{\vartheta_{12}E_2}{(1-\vartheta_{12}\vartheta_{21})}, \frac{E_1}{2(1+\vartheta_{12})}, \frac{E_2}{(1-\vartheta_{12}\vartheta_{21})}\right)z^2dz$.

## 3 Analytical solutions of the biaxial buckling

In this work, it is assumed that all edges of each rectangular microplate are simply supported; thus, deflection and moment conditions in the classical boundary conditions can be given as

$$w_\varsigma(0,y)=w_\varsigma(L_x,y)=w_\varsigma(x,0)=w_\varsigma\left(x,L_y\right)=0\,,\quad \varsigma=1,2,\ldots,Q, \tag{17a}$$

$$M_{\varsigma xx}(0,y)=M_{\varsigma xx}(L_x,y)=M_{\varsigma yy}(x,0)=M_{\varsigma yy}\left(x,L_y\right)=0. \tag{17b}$$

Also, the non-classical boundary condition is expressed as [36,37]

$$w_\varsigma=0,\quad w_{\varsigma xx}=w_{\varsigma yy}=0,\quad w_{\varsigma xxxx}=w_{\varsigma yyyy}=w_{\varsigma xxyy}=0 \text{ at } x=0, L_x \text{ and } y=0, L_y. \tag{18}$$

The buckling equations solution due to the simply supported boundary conditions can be considered in the form of [38]

$$w_\varsigma(x,y)=\sum_{m=1}^{\infty}\sum_{n=1}^{\infty}\overline{W}_{\varsigma mn}\sin\left(\frac{m\pi}{L_x}x\right)\sin\left(\frac{n\pi}{L_y}y\right),\ \varsigma=1,2,\ldots,Q, \tag{19}$$

where $m$ and $n$ demonstrate half wave numbers. Also, $\overline{W}_{\varsigma mn}$ denotes the amplitude for the $\varsigma$-th orthotropic microplate. By employing the assumed solution (19) into Eq. (16) and then applying non-dimensional parameters, we have a new non-dimensional homogeneous system of $Q$ algebraic equations as below:

$$\alpha\overline{W}_{\varsigma-1mn}+\beta\overline{W}_{\varsigma mn}+\alpha\overline{W}_{\varsigma+1mn}=0, \tag{20}$$

where

$$\alpha = -K - K_1((m\pi)^2 + R^2(n\pi)^2), \tag{21a}$$

$$\begin{aligned}\beta = &\left(1 + \frac{6\,(1-\vartheta_{12})}{h^2}\left(2{l_0}^2 + \frac{8}{15}{l_1}^2 + {l_2}^2\right)\right)(m\pi)^4 \\ &+ \left(2\,(Z_{12} + 2Z_{66}) + \frac{6\,(1-\vartheta_{12})}{h^2}\left(4{l_0}^2 + \frac{16}{15}{l_1}^2 + 2{l_2}^2\right)\right)(m\pi)^2(n\pi)^2R^2 \\ &+ \left(Z_{22} + \frac{6\,(1-\vartheta_{12})}{h^2}\left(2{l_0}^2 + \frac{8}{15}{l_1}^2 + {l_2}^2\right)\right)(n\pi)^4R^4 + 6\,(1-\vartheta_{12})\left(\frac{{l_0}^2}{6} + \frac{{l_1}^2}{15}\right)\frac{(m\pi)^6}{{L_x}^2} \\ &+ 6\,(1-\vartheta_{12})\left(\frac{{l_0}^2}{2} + \frac{{l_1}^2}{5}\right)\frac{(m\pi)^4(n\pi)^2}{{L_y}^2} + 6\,(1-\vartheta_{12})\left(\frac{{l_0}^2}{2} + \frac{{l_1}^2}{5}\right) \\ &\times \frac{(m\pi)^2(n\pi)^4R^2}{{L_y}^2} + 6\,(1-\vartheta_{12})\left(\frac{{l_0}^2}{6} + \frac{{l_1}^2}{15}\right)\frac{(n\pi)^6R^4}{{L_y}^2} - \overline{N}\left((m\pi)^2 + \lambda R^2(n\pi)^2\right) \\ &+ 2K + 2K_1\left((m\pi)^2 + R^2(n\pi)^2\right),\end{aligned} \tag{21b}$$

where the non-dimensional parameters implemented in Eq. (21) are illustrated as follows:

$$Z_{12} = \frac{D_{12}}{D_{11}}, Z_{66} = \frac{D_{66}}{D_{11}}, Z_{22} = \frac{D_{22}}{D_{11}}, R = \frac{L_x}{L_y}, K = \frac{KL_x^4}{D_{11}}, K_1 = \frac{k_1L_x^2}{D_{11}}, \overline{N} = -\frac{N_x^0L_x^2}{D_{11}}. \tag{22}$$

### 3.1 Clamped-Chain system

As seen in Fig. 1b, we assumed that the first and last microplates in the multi-microplate system are connected with a fixed surface by a Pasternak elastic medium. Thus, we introduce the following matrix form of the algebraic equation (20):

$$\begin{bmatrix} \beta & \alpha & 0 & \cdots & 0 & 0 & 0 & \cdots & 0 & 0 & 0 \\ \alpha & \beta & \alpha & \cdots & 0 & 0 & 0 & \cdots & 0 & 0 & 0 \\ \cdots & \cdots & \cdots & \cdots & \cdots & \cdots & \cdots & \cdots & \cdots & \cdots & \cdots \\ 0 & 0 & 0 & \cdots & \beta & \alpha & 0 & \cdots & 0 & 0 & 0 \\ 0 & 0 & 0 & \cdots & \alpha & \beta & \alpha & \cdots & 0 & 0 & 0 \\ 0 & 0 & 0 & \cdots & 0 & \alpha & \beta & \cdots & 0 & 0 & 0 \\ \cdots & \cdots & \cdots & \cdots & \cdots & \cdots & \cdots & \cdots & \cdots & \cdots & \cdots \\ 0 & 0 & 0 & \cdots & 0 & 0 & 0 & \cdots & \alpha & \beta & \alpha \\ 0 & 0 & 0 & \cdots & 0 & 0 & 0 & \cdots & 0 & \alpha & \beta \end{bmatrix} \begin{Bmatrix} \overline{W}_{1mn} \\ \overline{W}_{2mn} \\ \cdots \\ \overline{W}_{\varsigma-1mn} \\ \overline{W}_{\varsigma mn} \\ \overline{W}_{\varsigma+1mn} \\ \cdots \\ \overline{W}_{Q-1mn} \\ \overline{W}_{Qmn} \end{Bmatrix} = \begin{Bmatrix} 0 \\ 0 \\ \cdots \\ 0 \\ 0 \\ 0 \\ \cdots \\ 0 \\ 0 \end{Bmatrix}. \tag{23}$$

Also, the trigonometric method presented by Raskovic [39,40] and developed by Stojanović et al. [41] is exerted to achieve an explicit closed-form expression to predict size effects on the buckling load of OMMPS. According to the trigonometric approach, we consider the following solution of the amplitude of the $\varsigma$-th algebraic equation for the OMMPS as

$$\overline{W}_{\varsigma mn} = Y\cos\left(\varsigma\theta_{\mathrm{CC}}\right) + \mathrm{G}\sin\left(\varsigma\theta_{\mathrm{CC}}\right), \tag{24}$$

in which $Y$ and $G$ denote nonzero constants which should satisfy the boundary conditions and $\theta_{CC}$ is an unknown parameter. Substituting the solution (24) into the $\varsigma$-th equation of the OMMPS (23) leads to

$$Y\left(\alpha\cos\left(\left(\varsigma-1\right)\theta_{\mathrm{CC}}\right) + \beta\cos\left(\varsigma\theta_{\mathrm{CC}}\right) + \alpha\cos\left(\left(\varsigma+1\right)\theta_{\mathrm{CC}}\right)\right) = 0,\ \varsigma = 2, 3, \ldots, Q-1, \tag{25a}$$

$$G\left(\alpha\sin\left(\left(\varsigma-1\right)\theta_{\mathrm{CC}}\right) + \beta\sin\left(\varsigma\theta_{\mathrm{CC}}\right) + \alpha\sin\left(\left(\varsigma+1\right)\theta_{\mathrm{CC}}\right)\right) = 0\,,\quad \varsigma = 2, 3, \ldots, Q-1. \tag{25b}$$

After applying some trigonometric operations on Eq. (25), we have the following new form

$$Y\left(\beta + 2\alpha\cos\theta_{\mathrm{CC}}\right)\cos\left(\varsigma\theta_{\mathrm{CC}}\right) = 0,\ \varsigma = 2, 3, \ldots, Q-1, \tag{26a}$$

$$G\left(\beta + 2\alpha\cos\theta_{\mathrm{CC}}\right)\sin\left(\varsigma\theta_{\mathrm{CC}}\right) = 0,\ \varsigma = 2, 3, \ldots, Q-1. \tag{26b}$$

It should be noted that in Eq. (26), $Y$, $G$, $\cos(\varsigma\theta_{CC})$ and $\sin(\varsigma\theta_{CC})$ cannot be equal to zero because then $\overline{W}_{\varsigma mn}$ would be zero; thus, we obtain the following buckling load equation:

$$\beta + 2\alpha\cos\theta_{CC} = 0. \tag{27}$$

Also, to obtain unknown parameter $\theta_{CC}$, we apply the first and the last equations of the OMMPS of Eq. (23) satisfied with a solution (24). For this purpose, the following relations can be assumed:

$$\overline{W}_{1mn} = Y\cos(\theta_{CC}) + G\sin(\theta_{CC}), \tag{28a}$$

$$\overline{W}_{2mn} = Y\cos(2\theta_{CC}) + G\sin(2\theta_{CC}), \tag{28b}$$

and

$$\overline{W}_{Q-1mn} = Y\cos((Q-1)\theta_{CC}) + G\sin((Q-1)\theta_{CC}), \tag{29a}$$

$$\overline{W}_{Qmn} = Y\cos(Q\theta_{CC}) + G\sin(Q2\theta_{CC}). \tag{29b}$$

Substituting Eq. (28) into the first equation of the system (23) and Eq. (29) into the $Q$-th equation of the system (23) yields

$$Y\{\beta\cos\theta_{CC} + \alpha\cos2\theta_{CC}\} + G\{\beta\sin\theta_{CC} + \alpha\sin2\theta_{CC}\} = 0, \tag{30a}$$

$$Y\{\beta\cos(Q\theta_{CC}) + \alpha\cos((Q-1)\theta_{CC})\} + G\{\beta\sin(Q\theta_{CC}) + \alpha\sin((Q-1)\theta_{CC})\} = 0. \tag{30b}$$

According to the non-trivial solutions acquired from the constants $Y$ and $G$ of Eq. (30) and after some trigonometric operations, the following trigonometric equation is expressed:

$$\begin{vmatrix} 1 & 0 \\ \cos((Q+1)\theta_{CC}) & \sin((Q+1)\theta_{CC}). \end{vmatrix} = 0. \tag{31}$$

The unknown parameter $\theta_{CC}$ can be obtained by taking the determinant of Eq. (31) as

$$\sin((Q+1)\theta_{CC}) = 0 \Rightarrow \theta_{CC} = \frac{r\pi}{Q+1}, \quad r = 1, 2, \ldots, Q. \tag{32}$$

Applying $\theta_{CC}$ from Eq. (32) into Eq. (27), a non-dimensional explicit closed-form expression for buckling load of the multi-microplate system can be obtained as

$$\overline{N}_{CC} = \frac{N_{CC}}{M_{CC}}, \tag{33a}$$

$$\begin{aligned} N_{CC} = {} & \left(1 + \frac{6(1-\vartheta_{12})}{h^2}\left(2l_0^2 + \frac{8}{15}l_1^2 + l_2^2\right)\right) \\ & (m\pi)^4 + \left(2(Z_{12} + 2Z_{66}) + \frac{6(1-\vartheta_{12})}{h^2}\left(4l_0^2 + \frac{16}{15}l_1^2 + 2l_2^2\right)\right) \\ & (m\pi)^2(n\pi)^2R^2 + \left(Z_{22} + \frac{6(1-\vartheta_{12})}{h^2}\left(2l_0^2 + \frac{8}{15}l_1^2 + l_2^2\right)\right) \\ & (n\pi)^4R^4 + 6(1-\vartheta_{12})\left(\frac{l_0^2}{6} + \frac{l_1^2}{15}\right) \\ & \frac{(m\pi)^6}{L_x^2} + 6(1-\vartheta_{12})\left(\frac{l_0^2}{2} + \frac{l_1^2}{5}\right) \\ & \frac{(m\pi)^4(n\pi)^2}{L_y^2} + 6(1-\vartheta_{12})\left(\frac{l_0^2}{2} + \frac{l_1^2}{5}\right) \\ & \frac{(m\pi)^2(n\pi)^4R^2}{L_y^2} + 6(1-\vartheta_{12}) \\ & \left(\frac{l_0^2}{6} + \frac{l_1^2}{15}\right)\frac{(n\pi)^6R^4}{L_y^2} + 2K(1-\cos\theta_C C) + 2K_1((\mathrm{m}\pi)^2 + R^2(\mathrm{n}\pi)^2)(1-\cos\theta_{CC}), \end{aligned} \tag{33b}$$

$$M_{CC} = \left((m\pi)^2 + \lambda R^2(n\pi)^2\right). \tag{33c}$$

### 3.2 Cantilever-Chain system

In this case of chain boundary conditions, the bottom microplate in the multi-microplate system is connected to the fixed surface by a Pasternak elastic medium, while the top microplate in the multi-microplate system is free, see Fig. 1c. The matrix form of the algebraic equation (20) compatible with the "Cantilever-Chain" system can be obtained as

$$\begin{bmatrix} \beta & \alpha & 0 & \cdots & 0 & 0 & 0 & \cdots & 0 & 0 & 0 \\ \alpha & \beta & \alpha & \cdots & 0 & 0 & 0 & \cdots & 0 & 0 & 0 \\ \cdots & \cdots & \cdots & \cdots & \cdots & \cdots & \cdots & \cdots & \cdots & \cdots & \cdots \\ 0 & 0 & 0 & \cdots & \beta & \alpha & 0 & \cdots & 0 & 0 & 0 \\ 0 & 0 & 0 & \cdots & \alpha & \beta & \alpha & \cdots & 0 & 0 & 0 \\ 0 & 0 & 0 & \cdots & 0 & \alpha & \beta & \cdots & 0 & 0 & 0 \\ \cdots & \cdots & \cdots & \cdots & \cdots & \cdots & \cdots & \cdots & \cdots & \cdots & \cdots \\ 0 & 0 & 0 & \cdots & 0 & 0 & 0 & \cdots & \alpha & \beta & \alpha \\ 0 & 0 & 0 & \cdots & 0 & 0 & 0 & \cdots & 0 & \alpha & \beta+\alpha \end{bmatrix} \begin{Bmatrix} \overline{W}_{1mn} \\ \overline{W}_{2mn} \\ \cdots \\ \overline{W}_{\varsigma-1mn} \\ \overline{W}_{\varsigma mn} \\ \overline{W}_{\varsigma+1mn} \\ \cdots \\ \overline{W}_{Q-1mn} \\ \overline{W}_{Qmn} \end{Bmatrix} = \begin{Bmatrix} 0 \\ 0 \\ \cdots \\ 0 \\ 0 \\ 0 \\ \cdots \\ 0 \\ 0 \end{Bmatrix}. \tag{34}$$

In order to determine the closed form of the buckling load of the OMMPS for the "Cantilever-Chain" system, by applying the assumed solution (24) into the $\varsigma$-th algebraic equation of system (34), the following buckling load expression will be achieved:

$$\beta + 2\alpha\cos\theta_{\mathrm{CaC}} = 0, \tag{35}$$

where $\theta_{\mathrm{CaC}}$ is the unknown parameter for the "Cantilever-Chain" system. Applying the same steps that were carried out in the "Clamped-Chain" system, the unknown parameter $\theta$CaC will be obtained as

$$\cos\left(\left(\frac{2Q+1}{2}\right)\theta_{\mathrm{CaC}}\right) = 0 \Rightarrow \theta_{\mathrm{CaC}} = \frac{(2r-1)\,\pi}{2Q+1}, \quad r = 1, 2, \ldots, Q. \tag{36}$$

The dimensionless closed-form expression for the buckling load of the OMMPS for the "Cantilever-Chain" system can be obtained by inserting relation (36) into Eq. (35) as

$$\overline{N}_{\mathrm{CaC}} = \frac{N_{\mathrm{CaC}}}{M_{\mathrm{CaC}}}, \tag{37a}$$

$$\begin{aligned} N_{\mathrm{CaC}} = {} & \left(1 + \frac{6\,(1-\vartheta_{12})}{h^2}\left(2l_0^2 + \frac{8}{15}l_1^2 + l_2^2\right)\right)(m\pi)^4 \\ & + \left(2\,(Z_{12}+2Z_{66}) + \frac{6\,(1-\vartheta_{12})}{h^2}\left(4l_0^2 + \frac{16}{15}l_1^2 + 2l_2^2\right)\right)(m\pi)^2(n\pi)^2R^2 \\ & + \left(Z_{22} + \frac{6\,(1-\vartheta_{12})}{h^2}\left(2l_0^2 + \frac{8}{15}l_1^2 + l_2^2\right)\right)(n\pi)^4R^4 \\ & + 6\,(1-\vartheta_{12})\left(\frac{l_0^2}{6} + \frac{l_1^2}{15}\right)\frac{(m\pi)^6}{L_x^2} + 6\,(1-\vartheta_{12})\left(\frac{l_0^2}{2} + \frac{l_1^2}{5}\right)\frac{(m\pi)^4(n\pi)^2}{L_y^2} \\ & + 6\,(1-\vartheta_{12})\left(\frac{l_0^2}{2} + \frac{l_1^2}{5}\right)\frac{(m\pi)^2(n\pi)^4R^2}{L_y^2} + 6\,(1-\vartheta_{12})\left(\frac{l_0^2}{6} + \frac{l_1^2}{15}\right)\frac{(n\pi)^6R^4}{L_y^2} \\ & + 2K\,(1-\cos\theta_{\mathrm{CaC}}) + 2K_1\left((m\pi)^2 + R^2\,(n\pi)^2\right)(1-\cos\theta_{\mathrm{CaC}}), \end{aligned} \tag{37b}$$

$$M_{\mathrm{CaC}} = \left((m\pi)^2 + \lambda R^2\,(n\pi)^2\right). \tag{37c}$$

### 3.3 Free-Chain system

In this case of chain boundary conditions, it is considered that the first and last microplates are not connected with the fixed surface. The matrix form of the algebraic equation (20) compatible with the "Free-Chain" system can be presented as

$$\begin{bmatrix} \beta+\alpha & \alpha & 0 & \cdots & 0 & 0 & 0 & \cdots & 0 & 0 & 0 \\ \alpha & \beta & \alpha & \cdots & 0 & 0 & 0 & \cdots & 0 & 0 & 0 \\ \cdots & \cdots & \cdots & \cdots & \cdots & \cdots & \cdots & \cdots & \cdots & \cdots & \cdots \\ 0 & 0 & 0 & \cdots & \beta & \alpha & 0 & \cdots & 0 & 0 & 0 \\ 0 & 0 & 0 & \cdots & \alpha & \beta & \alpha & \cdots & 0 & 0 & 0 \\ 0 & 0 & 0 & \cdots & 0 & \alpha & \beta & \cdots & 0 & 0 & 0 \\ \cdots & \cdots & \cdots & \cdots & \cdots & \cdots & \cdots & \cdots & \cdots & \cdots & \cdots \\ 0 & 0 & 0 & \cdots & 0 & 0 & 0 & \cdots & \alpha & \beta & \alpha \\ 0 & 0 & 0 & \cdots & 0 & 0 & 0 & \cdots & 0 & \alpha & \beta+\alpha \end{bmatrix} \begin{Bmatrix} \overline{W}_{1mn} \\ \overline{W}_{2mn} \\ \cdots \\ \overline{W}_{\varsigma-1mn} \\ \overline{W}_{\varsigma mn} \\ \overline{W}_{\varsigma+1mn} \\ \cdots \\ \overline{W}_{Q-1mn} \\ \overline{W}_{Qmn} \end{Bmatrix} = \begin{Bmatrix} 0 \\ 0 \\ \cdots \\ 0 \\ 0 \\ 0 \\ \cdots \\ 0 \\ 0 \end{Bmatrix}. \tag{38}$$

Following the steps implemented to achieve the closed form for the buckling load in the previous sections, substituting the assumed solution (24) into the $\varsigma$-th equation of system (38), we have

$$\beta + 2\alpha\cos\theta_{FC} = 0, \tag{39}$$

where $\theta_{FC}$ is the unknown parameter related to "Free-Chain," which is obtained from the first and last equation of system (38) as follows:

$$\sin(Q\theta_{FC}) = 0 \Rightarrow \theta_{CaC} = \frac{r\pi}{Q}, \quad r = 0, 1, 2, \ldots, Q-1. \tag{40}$$

A closed-form expression for the buckling load of the OMMPS for the "Free-Chain" state is achieved by substituting relation (40) into Eq. (39) as

$$\overline{N}_{FC} = \frac{N_{FC}}{M_{FC}}, \tag{41a}$$

$$\begin{aligned} N_{FC} = {} & \left(1 + \frac{6(1-\vartheta_{12})}{h^2}\left(2{l_0}^2 + \frac{8}{15}{l_1}^2 + {l_2}^2\right)\right)(m\pi)^4 \\ & + \left(2(Z_{12} + 2Z_{66}) + \frac{6(1-\vartheta_{12})}{h^2}\left(4{l_0}^2 + \frac{16}{15}{l_1}^2 + 2{l_2}^2\right)\right)(m\pi)^2(n\pi)^2R^2 \\ & + \left(Z_{22} + \frac{6(1-\vartheta_{12})}{h^2}\left(2{l_0}^2 + \frac{8}{15}{l_1}^2 + {l_2}^2\right)\right) \\ & \times (n\pi)^4R^4 + 6(1-\vartheta_{12})\left(\frac{{l_0}^2}{6} + \frac{{l_1}^2}{15}\right)\frac{(m\pi)^6}{{L_x}^2} + 6(1-\vartheta_{12})\left(\frac{{l_0}^2}{2} + \frac{{l_1}^2}{5}\right)\frac{(m\pi)^4(n\pi)^2}{{L_y}^2} \\ & + 6(1-\vartheta_{12})\left(\frac{{l_0}^2}{2} + \frac{{l_1}^2}{5}\right)\frac{(m\pi)^2(n\pi)^4R^2}{{L_y}^2} + 6(1-\vartheta_{12})\left(\frac{{l_0}^2}{6} + \frac{{l_1}^2}{15}\right)\frac{(n\pi)^6R^4}{{L_y}^2} + 2K(1-\cos\theta_{FC}) \\ & + 2K_1\left((m\pi)^2 + R^2(n\pi)^2\right)(1-\cos\theta_{FC}), \end{aligned} \tag{41b}$$

$$M_{FC} = \left((m\pi)^2 + \lambda R^2(n\pi)^2\right). \tag{41c}$$

## 4 Numerical examples and discussion

### 4.1 Comparison studies

In order to test the dependability of the formulation derived in this paper, several comparison studies are carried out to compare with existing data in the literature. Firstly, we have considered a state that the number of orthotropic microplates $Q$ tends to infinity. Based on this case, we propose the critical buckling load of the system as

**Table 1** Comparison of the critical buckling loads ($10^4$N/m) of OMMPS based on MSGT ($m = 1, n = 1$).

| $\frac{L_x}{h}$ | Current | Ref. [42] |
|---|---|---|
| 5 | 3.616 | 3.616 |
| 10 | 0.873 | 0.873 |
| 15 | 0.385 | 0.385 |
| 20 | 0.216 | 0.216 |

$$\overline{\mathrm{N}}_{\mathrm{Q}\to\infty}, = \frac{N}{M}, \tag{42a}$$

$$\begin{aligned} N = & \left(1+\frac{6\left(1-\vartheta_{12}\right)}{h^2}\left(2{l_0}^2+\frac{8}{15}{l_1}^2+{l_2}^2\right)\right) \\ & \times (m\pi)^4+\left(2\left(Z_{12}+2Z_{66}\right)+\frac{6\left(1-\vartheta_{12}\right)}{h^2}\left(4{l_0}^2+\frac{16}{15}{l_1}^2+2{l_2}^2\right)\right)(m\pi)^2 \\ & \times (n\pi)^2R^2+\left(Z_{22}+\frac{6\left(1-\vartheta_{12}\right)}{h^2}\left(2{l_0}^2+\frac{8}{15}{l_1}^2+{l_2}^2\right)\right)(n\pi)^4R^4 \\ & +6\left(1-\vartheta_{12}\right)\left(\frac{{l_0}^2}{6}+\frac{{l_1}^2}{15}\right)\frac{(m\pi)^6}{{L_x}^2}+6\left(1-\vartheta_{12}\right)\left(\frac{{l_0}^2}{2}+\frac{{l_1}^2}{5}\right)\frac{(m\pi)^4(n\pi)^2}{{L_y}^2} \\ & +6\left(1-\vartheta_{12}\right)\left(\frac{{l_0}^2}{2}+\frac{{l_1}^2}{5}\right)\frac{(m\pi)^2(n\pi)^4R^2}{{L_y}^2}+6\left(1-\vartheta_{12}\right)\left(\frac{{l_0}^2}{6}+\frac{{l_1}^2}{15}\right)\frac{(n\pi)^6R^4}{{L_y}^2}, \end{aligned} \tag{42b}$$

$$M = \left((m\pi)^2+\lambda R^2(n\pi)^2\right). \tag{42c}$$

It is found from Eq. (42) that when the number of the microplate of the system tends to infinity, the effect of the Pasternak elastic medium on the buckling load of the system vanishes and the buckling behavior is similar to the buckling behavior of a single microplate. After proposing the critical buckling load in the above form, a comparison between critical buckling loads obtained for a single isotropic microplate based on MSGT as a function of different length to thickness with those obtained by Akgöz and Civalek [42] is shown in Table 1. After briefly reviewing the demonstrated data in Table 1, the dependability of our formulation will be determined.

In another comparison study, we analytically verified the accuracy of our formulation obtained using the trigonometric method for a case of chain systems suggested in this paper such as the "Cantilever-Chain" system. By taking $Q$ =1 in the buckling load presented in Eq. (37), we have an orthotropic microplate resting on a Pasternak elastic foundation. Thus, Eq. (37) can be reformulated for this state as follows:

$$\overline{N}_{\mathrm{CaC},Q=1} = \frac{N_{\mathrm{CaC}}}{M_{\mathrm{CaC}}}, \tag{43a}$$

$$\begin{aligned} N_{\mathrm{CaC},Q=1} = & \left(1+\frac{6\left(1-\vartheta_{12}\right)}{h^2}\left(2{l_0}^2+\frac{8}{15}{l_1}^2+{l_2}^2\right)\right)(m\pi)^4 \\ & +\left(2\left(Z_{12}+2Z_{66}\right)+\frac{6\left(1-\vartheta_{12}\right)}{h^2}\left(4{l_0}^2+\frac{16}{15}{l_1}^2+2{l_2}^2\right)\right) \\ & \times (m\pi)^2(n\pi)^2R^2+\left(Z_{22}+\frac{6\left(1-\vartheta_{12}\right)}{h^2}\left(2{l_0}^2+\frac{8}{15}{l_1}^2+{l_2}^2\right)\right) \\ & \times (n\pi)^4R^4+6\left(1-\vartheta_{12}\right)\left(\frac{{l_0}^2}{6}+\frac{{l_1}^2}{15}\right)\frac{(m\pi)^6}{{L_x}^2} \\ & +6\left(1-\vartheta_{12}\right)\left(\frac{{l_0}^2}{2}+\frac{{l_1}^2}{5}\right) \\ & \times\frac{(m\pi)^4(n\pi)^2}{{L_y}^2}+6\left(1-\vartheta_{12}\right)\left(\frac{{l_0}^2}{2}+\frac{{l_1}^2}{5}\right)\frac{(m\pi)^2(n\pi)^4R^2}{{L_y}^2} \\ & +6\left(1-\vartheta_{12}\right)\left(\frac{{l_0}^2}{6}+\frac{{l_1}^2}{15}\right) \end{aligned}$$

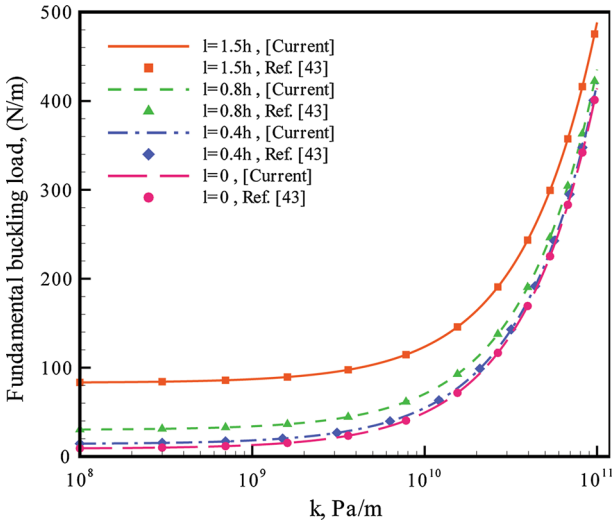


**Fig. 2** Comparison of the buckling loads of OMMPS for "Cantilever-Chain" system based on MCST ($Q = 1$)

$$\times \frac{(n\pi)^6 R^4}{{L_y}^2} + K + K_1 \left((m\pi)^2 + R^2(n\pi)^2\right), \tag{43b}$$

$$M_{\mathrm{CaC},Q=1} = \left((m\pi)^2 + \lambda R^2(n\pi)^2\right). \tag{43c}$$

Buckling loads predicted by MCST for isotropic microplate resting on the elastic medium are plotted in Fig. 2 along with those reported previously by Akgöz and Civalek [43], and a good agreement is found.

Finally, to confirm the obtained solution for the buckling load, analytical solutions of the homogenous set of equations (Eqs. (33), (37) and (41)) are compared to the numerical solution of the same set of equations (Eqs. (23), (34) and (38)) and tabulated in Table 2. Material properties and geometrical characteristics applied in this section and the following sections are supposed as [24,44]

$$\begin{aligned} &E_1 = 2.473\mathrm{TPa},\ E_2 = 2.433\mathrm{TPa},\ \vartheta_{12} = \vartheta_{21} = 0.197,\ h = 17.6\mu\mathrm{m},\ L_x = L_y = 10h, \\ &l_0 = l_1 = l_2 = 0.1h,\ K = 100,\ K_1 = 20,\ R = 1, \lambda = 1, m = n = 1 \end{aligned} \tag{44}$$

It can be seen from Table 2 that the values of the buckling load extracted from the exact solution and those obtained from the numerical solution are in good agreement for the three different boundary conditions, which verifies the accuracy of the present solution. It is notable that in the "Free-Chain" system the buckling load for $r = 0$ is independent of the number of microplates. Also, by increasing the number of microplates, the first buckling load tends to the critical buckling load of the system for both the "Clamped-Chain" and the "Cantilever-Chain" systems.

## 4.2 Benchmark results

The effect of thickness and material length scale parameter on the critical buckling load is investigated in Fig. 3. The critical buckling load is plotted versus the thickness of a single orthotropic plate for different values of material length scale parameters $l_0 = l_1 = l_2$. The figure obviously elucidates that increasing the value of the thickness causes a decrease of the critical buckling load toward the results of the classical theory (CT) ($l_0 = l_1 = l_2 = 0$). Also, an increase in the value of the independent material length scale parameters leads to greater critical buckling load.

The variation of non-dimensional buckling load versus thickness-to-material length scale parameter ratio is shown in Fig. 4 for three boundary conditions and four different numbers of plates by considering $r = 1$. Also, the separate influence of the orthotropic and isotropic materials on the buckling load is demonstrated. As shown in the figure, an increase in the thickness-to-material length scale parameter results in a significant decrease in buckling load. Furthermore, it is seen that dimensionless buckling load of the multi-isotropic microplate is

**Table 2** Comparison study of analytical and numerical solutions for non-dimensional buckling load of the OMMPS based on different chain systems.

| Number of plates | | "Free-Chain" system | | "Cantilever -Chain" system | | "Clamped-Chain" system | |
|---|---|---|---|---|---|---|---|
| | | N.S.[£] of Eq. (38) | A.S.[§] of Eq. (41) | N.S.[£] of Eq. (34) | A.S.[§] of Eq. (37) | N.S.[£] of Eq. (23) | A.S.[§] of Eq. (33) |
| $Q = 2$ | 1 | 23.03484985 | 23.03484986 | 32.60923250 | 32.60923251 | 48.10090904 | 48.10090904 |
| | 2 | 73.16696820 | 73.16696822 | 88.65864474 | 88.65864472 | 98.23302738 | 98.23302744 |
| $Q = 3$ | 1 | 23.03484984 | 23.03484986 | 27.99949030 | 27.99949030 | 37.71820738 | 37.71820738 |
| | 2 | 48.10090907 | 48.10090904 | 62.01152238 | 62.01152244 | 73.16696817 | 73.16696822 |
| | 3 | 98.23302736 | 98.23302744 | 104.4238328 | 104.4238328 | 108.6157291 | 108.6157290 |
| $Q = 5$ | 1 | 23.03485000 | 23.03484986 | 25.06555290 | 25.06555290 | 29.75128020 | 29.75128017 |
| | 2 | 32.60923187 | 32.60923251 | 40.33741218 | 40.33741240 | 48.10090856 | 48.10090904 |
| | 3 | 57.67529325 | 57.67529171 | 66.03242477 | 66.03242391 | 73.16696991 | 73.16696822 |
| | 4 | 88.65864277 | 88.65864472 | 93.99260158 | 93.99260279 | 98.23302509 | 98.23302744 |
| | 5 | 113.7247048 | 113.7247039 | 115.3407904 | 115.3407899 | 116.5826573 | 116.5826562 |
| $Q = 10$ | 1 | 23.03481663 | 23.03484986 | 23.59476288 | 23.59478420 | 25.06554939 | 25.06555290 |
| | 2 | 25.48857358 | 25.48849038 | 27.99957233 | 27.99949030 | 30.99317757 | 30.99314654 |
| | 3 | 32.60908507 | 32.60923251 | 36.41732925 | 36.41752502 | 40.33723223 | 40.33741240 |
| | 4 | 43.70038487 | 43.70004838 | 48.10123228 | 48.10090904 | 52.34223753 | 52.34133363 |
| | 5 | 57.67428896 | 57.67529171 | 62.01138644 | 62.01152244 | 66.02850095 | 66.03242391 |
| | 6 | 73.17015650 | 73.16696822 | 76.91242246 | 76.91334609 | 80.31443297 | 80.30151252 |
| | 7 | 88.65063474 | 88.65864472 | 91.48497266 | 91.48228766 | 93.96341123 | 93.99260279 |
| | 8 | 102.6472777 | 102.6338881 | 104.4201672 | 104.4238328 | 106.0395927 | 105.9965240 |
| | 9 | 113.7117672 | 113.7247039 | 114.5908245 | 114.5880682 | 115.3033317 | 115.3407899 |
| | 10 | 120.8505784 | 120.8454461 | 121.0709529 | 121.0718572 | 121.2822158 | 121.2683835 |

£ Numerical solutions
§ Analytical solutions

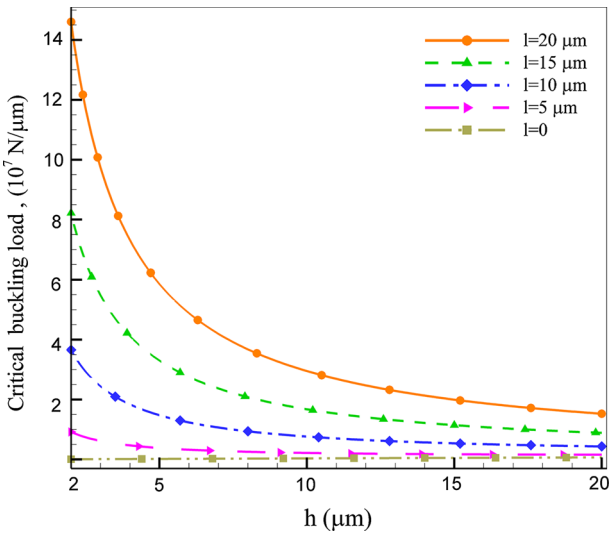


**Fig. 3** Variations of the critical buckling loads of the OMMPS as a function of plate thickness for various values of the independent material length scale parameters

always larger than for OMMPS. This is due to the fact that the isotropic properties of the plate make it more rigid than the orthotropic one.

In Fig. 5, a comparison is performed between buckling analysis based on MSGT and based on its reduced forms, modified couple stress theory and classical theory for different values of thickness-to-material length scale parameter ratio and a different number of plates. Here, we took $r = 1$ for all chain systems. All three material length scale parameters are the same for MSGT, i.e., $l_0 = l_1 = l_2$. Letting $l_0 = l_1 = 0$, this theory will be converted to the modified couple stress theory, and if all three parameters are taken to be zero, we will have the classical theory. The figure includes diagrams for three cases of boundary conditions. One can observe from the figure that the buckling load predicted by MSGT is larger than for both modified couple

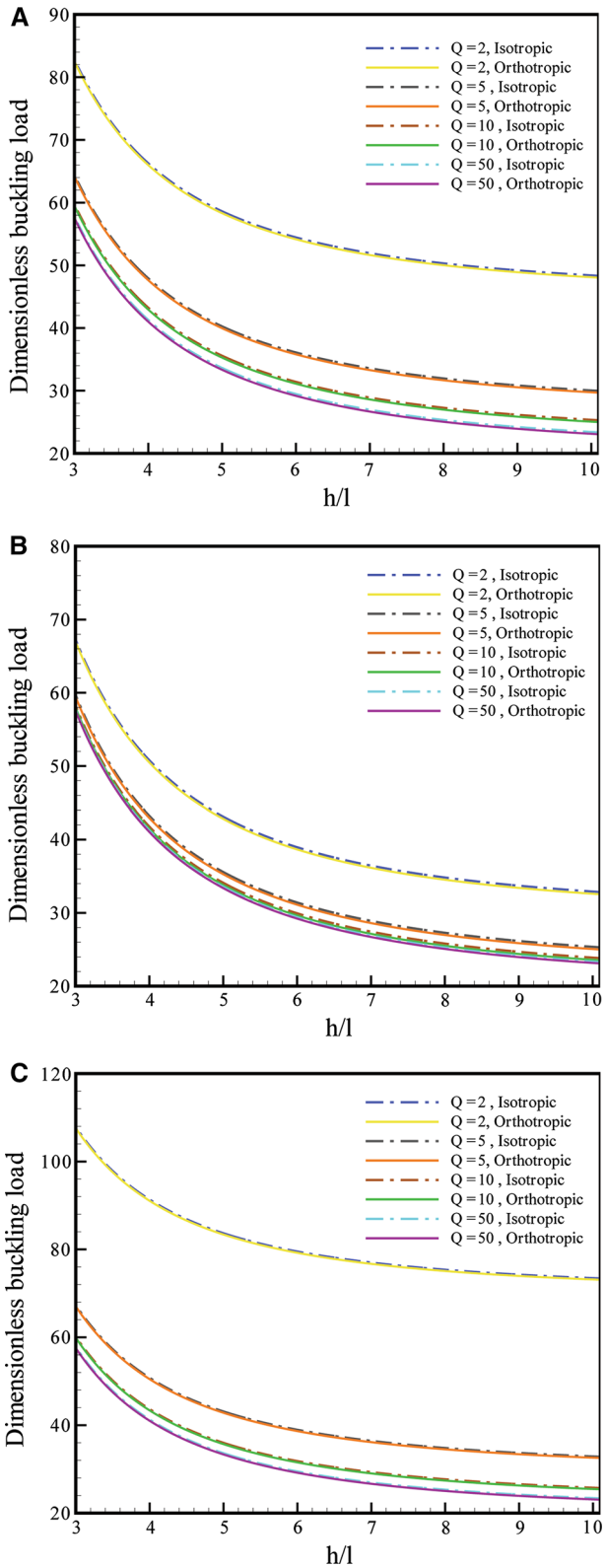


**Fig. 4** The separate influence of the orthotropic and isotropic materials on dimensionless buckling loads of OMMPS versus non-dimensional length scale parameter for different number of microplates, **a** "Clamped-Chain," **b**"Cantilever-Chain," **c** "Free-Chain"

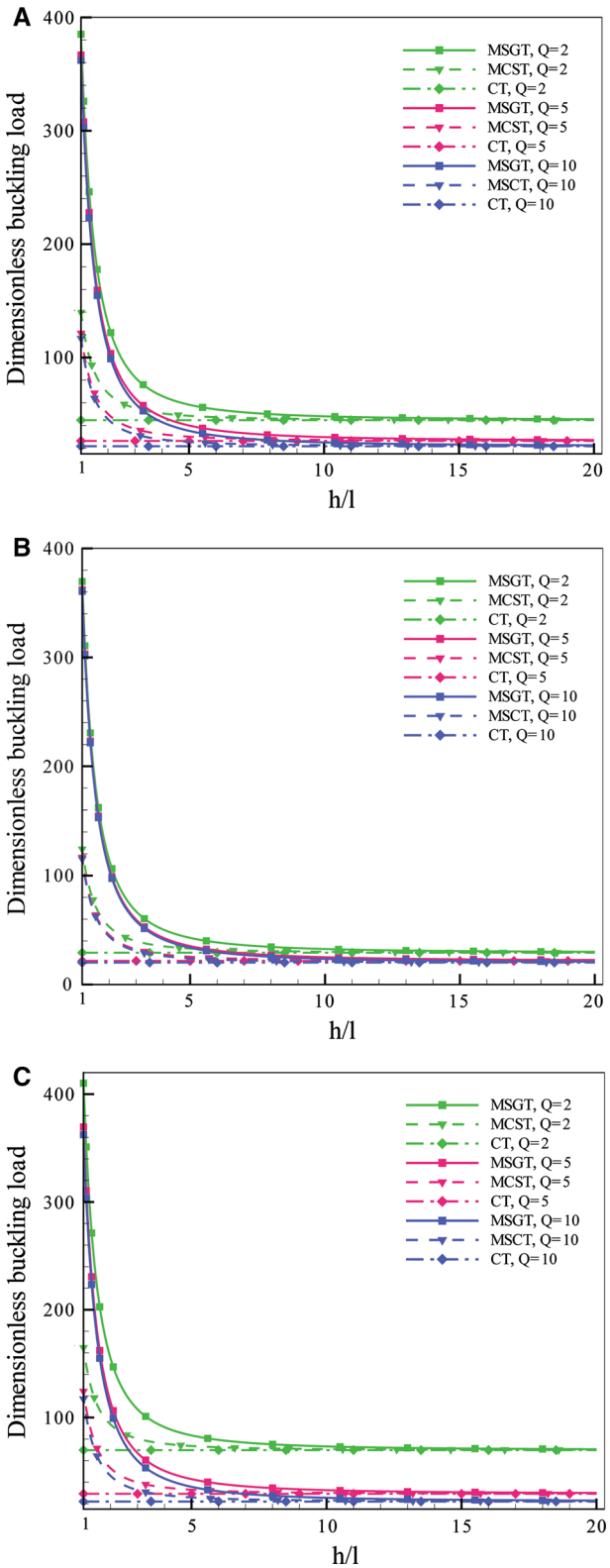


**Fig. 5** Variations of the dimensionless buckling loads of OMMPS predicted by MSGT, MCST and CT corresponding to various values of the non-dimensional length scale parameter and different number of microplates, **a** "Clamped-Chain," **b** "Cantilever-Chain," **c** "Free-Chain"

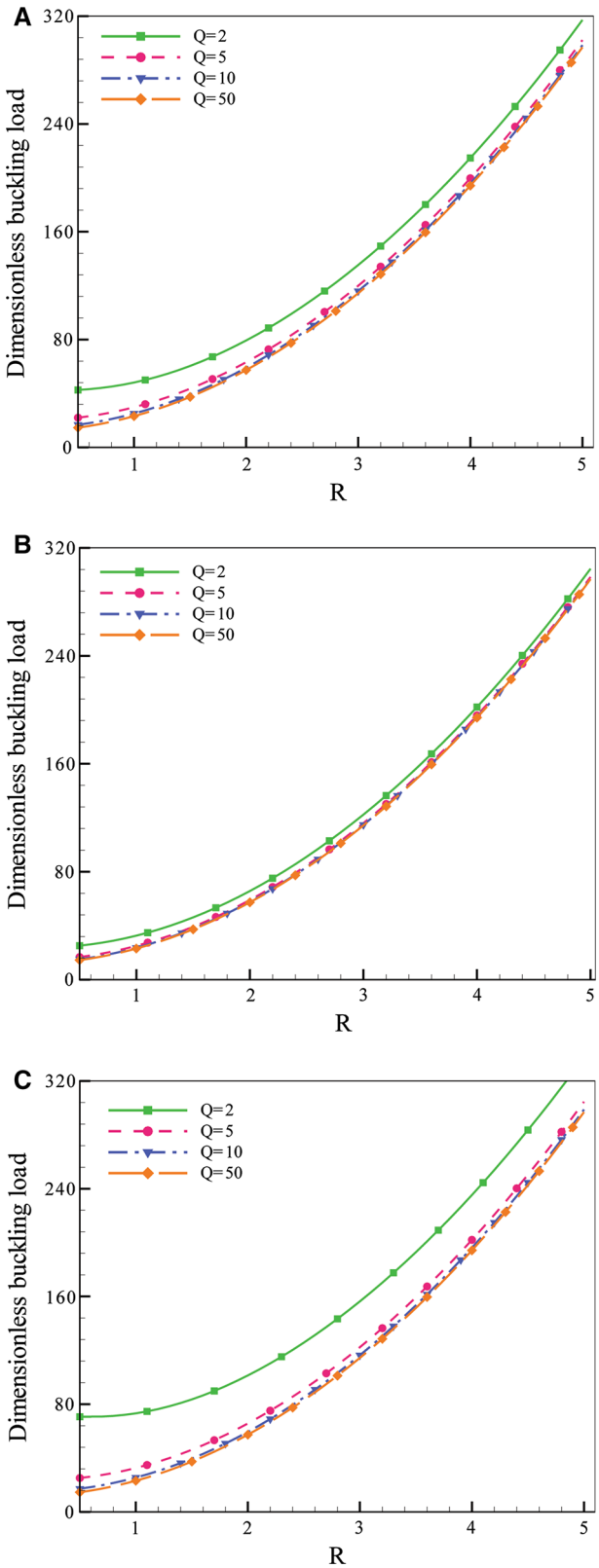


**Fig. 6** Variations of the dimensionless buckling loads of OMMPS against the aspect ratio for different number of microplates. **a** "Clamped-Chain," **b** "Cantilever-Chain," **c** "Free-Chain"

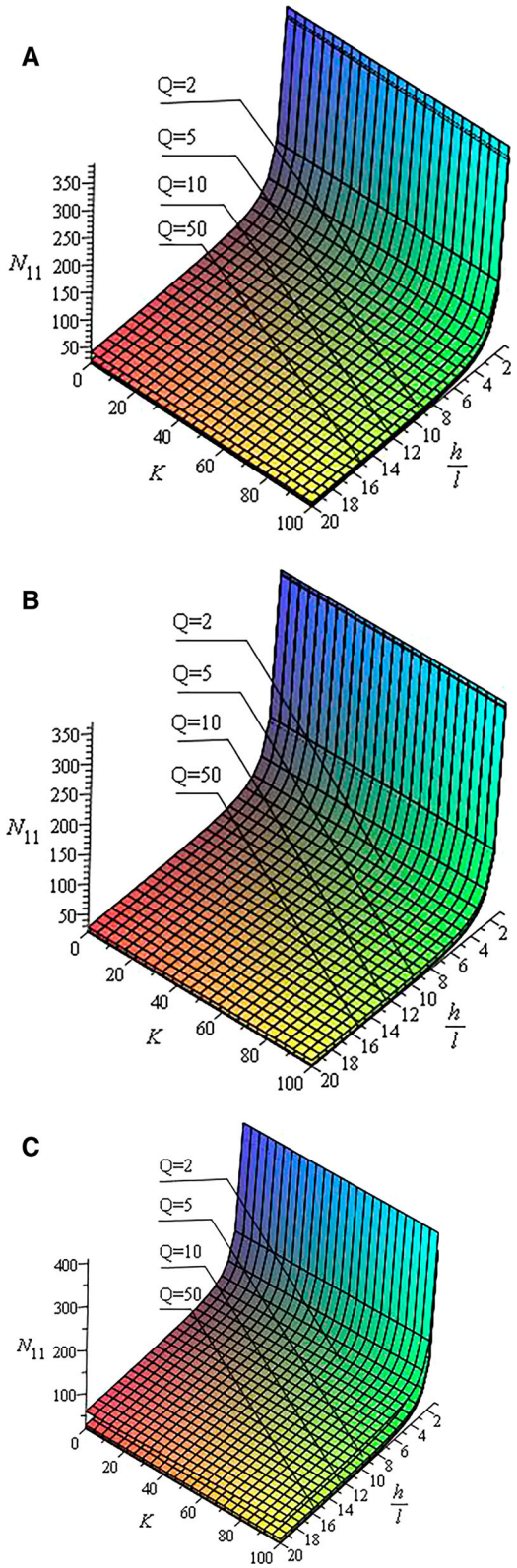


**Fig. 7** Variations of the dimensionless buckling loads of OMMPS against the non-dimensional transverse stiffness coefficient $K$ and the non-dimensional length scale parameter for different number of microplates. **a** "Clamped-Chain" **b** "Cantilever-Chain," **c**"Free-Chain"

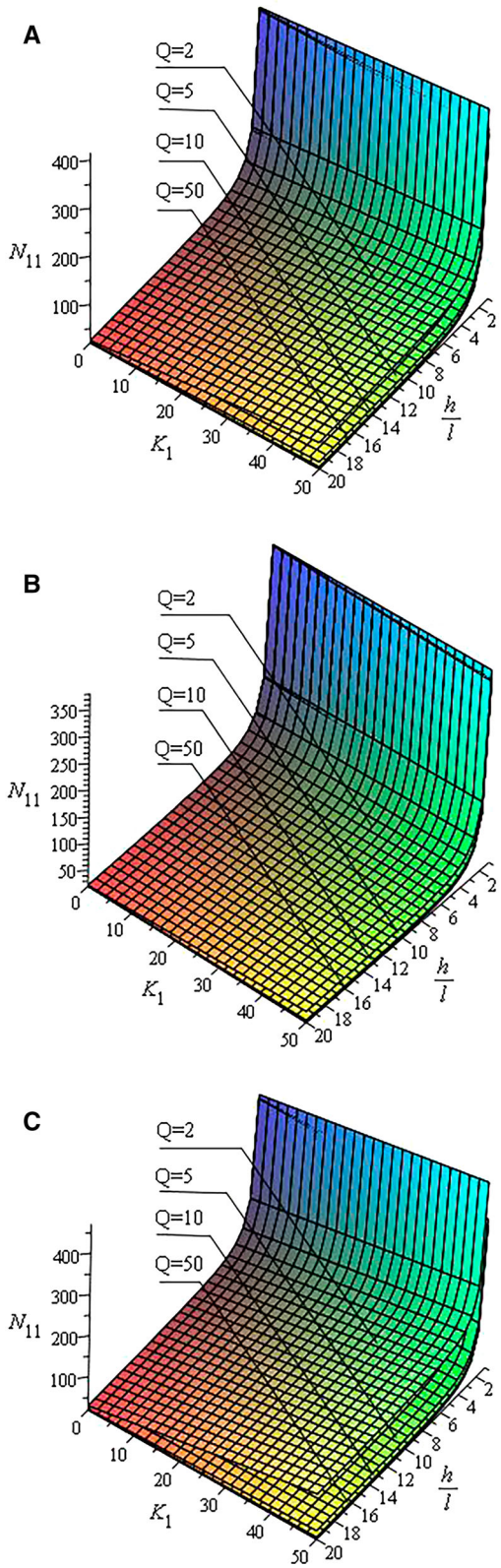


**Fig. 8** Variations of the dimensionless buckling loads of OMMPS against the non-dimensional shear stiffness coefficient $K_1$ and the non-dimensional length scale parameter for different number of microplates. **a** "Clamped-Chain," **b** "Cantilever-Chain," **c** "Free-Chain"

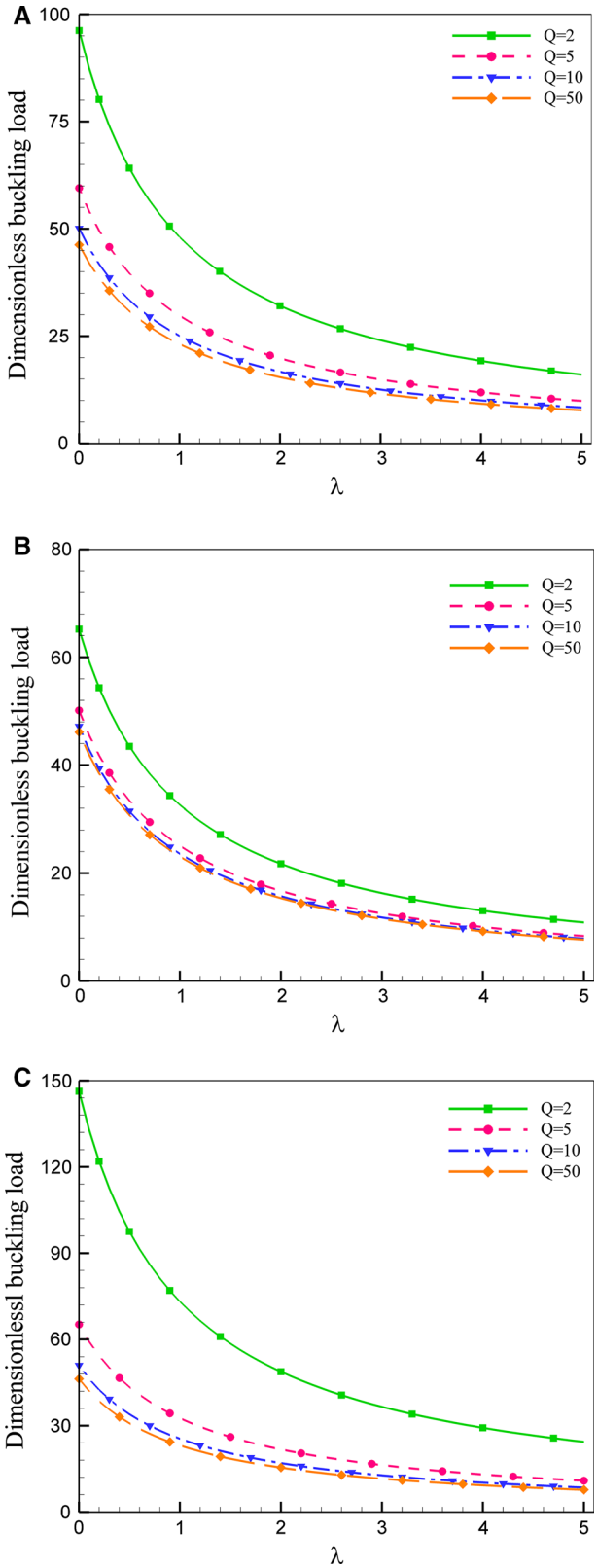


**Fig. 9** Effect of the axial force ratio on the dimensionless buckling loads of OMMPS for different number of microplates. **a** "Clamped-Chain," **b** "Cantilever-Chain," **c** "Free-Chain"

stress and classical theories. This is due to the higher bending rigidity of the plates in MSGT in comparison with the two other theories. Also it is seen that the difference between dimensionless buckling load obtained by MSGT, MCST and CT is negligible for higher values of dimensionless length scale parameter.

The effect of an increase of aspect ratio on buckling load for a different number of microplates and three boundary conditions is depicted in Fig. 6. Here, we took $r = 1$ for all chain systems. As can be seen from the diagrams (a), (b) and (c), the buckling load increases with increasing aspect ratio and decreases with increasing number of plates.

Figure 7 presents the effects of variations of transverse stiffness coefficient and thickness-to-material length scale parameter on the dimensionless buckling load. Here, we took $r = 1$ for all chain systems. It is obvious from the figure that the buckling load considerably decreases with increasing thickness-to-material length scale parameter and slightly increases with increasing transverse stiffness coefficient. The results reveal that there is a little difference between the buckling loads extracted by using the different set of boundary conditions. In Fig. 8, the same diagrams are plotted to exhibit the effects of variations of shear stiffness coefficient and thickness-to-material length scale parameter on the dimensionless buckling load. The figure illustrates that in the case of "Free-Chain" boundary condition the difference between the values of the buckling loads for different numbers of plates is larger than the two other boundary conditions.

Variation of the buckling load against the axial force ratio for the different set of boundary conditions is delineated in Fig. 9. Here, we took $r = 1$ for all chain systems. The compression ratio $\lambda = 0$ shows uniaxial compression. An increase in the axial force ratio leads to a reduction in the buckling load for all numbers of microplates. The results also demonstrate that the higher number of plates does not significantly affect the buckling load in the case of the "Cantilever-Chain" condition in comparison with the other chain conditions.

## 5 Conclusion

In the present paper, biaxial buckling behavior of an OMMPS embedded in a Pasternak elastic medium is investigated based on the MSGT and the Kirchhoff plate approach. It is assumed that the boundary conditions of all four edges of each microplate are simply supported. The governing equations and corresponding boundary conditions are derived using the principle of total potential energy. Explicit closed-form expressions for the buckling load of the OMMPS for different "chain" conditions, "Clamped-Chain," "Free-Chain" and "Cantilever-Chain," are proposed using Navier's method and the trigonometric method. Several comparison studies were carried out to check the accuracy of the obtained exact closed-form solutions. It is found from numerical results that the buckling load is significantly influenced by the number of microplates, the length scale parameter $\left(\frac{h}{l}\right)$, the aspect ratio and the microplate thickness. Also, we found that when the number of microplates in the OMMPS increases, the influence of the stiffness parameters of the Pasternak elastic medium on the buckling load decreases toward zero. Moreover, an increase in the microplate thickness causes the buckling load computed from MSGT and MCST to decrease toward the results of the classical approach for all three chain systems.

## Appendix

Substituting Equations (3), (6) and (8) into equation (14), $M_{xx}$, $M_{yy}$, $M_{xy}$, $\Lambda_{xxx}$, $\Lambda_{xxy}$, $\Lambda_{xyy}$ and $\Lambda_{yyy}$ are given in terms of the plate deflection as below:

$$M_{xx} = -\left\{\frac{E_1 h^3}{12\left(1-\vartheta_{12}\vartheta_{21}\right)} + \frac{E_1 h}{2\left(1+\vartheta_{12}\right)}\left(2l_0^2 + \frac{8}{15}l_1^2 + l_2^2\right)\right\}\frac{\partial^2 w_\varsigma}{\partial x^2} - \left\{\frac{\vartheta_{12}E_2 h^3}{12\left(1-\vartheta_{12}\vartheta_{21}\right)} + \frac{E_1 h}{2\left(1+\vartheta_{12}\right)}\left(2l_0^2 - \frac{2}{15}l_1^2 - l_2^2\right)\right\}\frac{\partial^2 w_\varsigma}{\partial y^2}, \tag{45a}$$

$$M_{yy} = -\left\{\frac{\vartheta_{12}E_2 h^3}{12\left(1-\vartheta_{12}\vartheta_{21}\right)} + \frac{E_1 h}{2\left(1+\vartheta_{12}\right)}\left(2l_0^2 - \frac{2}{15}l_1^2 + l_2^2\right)\right\}\frac{\partial^2 w_\varsigma}{\partial x^2} - \left\{\frac{E_1 h^3}{12\left(1-\vartheta_{12}\vartheta_{21}\right)} + \frac{E_1 h}{2\left(1+\vartheta_{12}\right)}\left(2l_0^2 + \frac{8}{15}l_1^2 - l_2^2\right)\right\}\frac{\partial^2 w_\varsigma}{\partial y^2}, \tag{45b}$$

$$M_{xy} = -\frac{E_1 \mathrm{h}}{2\,(1+\vartheta_{12})}\left\{\frac{h^2}{3}+4\left(\frac{l_1^2}{3}+l_2^2\right)\right\}\frac{\partial^2 w_\varsigma}{\partial x \partial y}, \tag{45c}$$

$$\Lambda_{xxx} = -\frac{E_1 h}{2\,(1+\vartheta_{12})}\left\{\left(\frac{l_0^2}{6}+\frac{l_1^2}{15}\right)\frac{\partial^3 w_\varsigma}{\partial x^3}+\left(\frac{l_0^2}{6}-\frac{l_1^2}{10}\right)\frac{\partial^3 w_\varsigma}{\partial x \partial y^2}\right\}, \tag{45d}$$

$$\Lambda_{xxy} = -\frac{E_1 h}{2\,(1+\vartheta_{12})}\left\{\left(\frac{l_0^2}{6}+\frac{2l_1^2}{5}\right)\frac{\partial^3 w_\varsigma}{\partial x^2 \partial y}+\left(\frac{l_0^2}{6}-\frac{l_1^2}{10}\right)\frac{\partial^3 w_\varsigma}{\partial y^3}\right\}, \tag{45e}$$

$$\Lambda_{xyy} = -\frac{E_1 h}{2\,(1+\vartheta_{12})}\left\{\left(\frac{l_0^2}{6}+\frac{2l_1^2}{5}\right)\frac{\partial^3 w_\varsigma}{\partial x \partial y^2}+\left(\frac{l_0^2}{6}-\frac{l_1^2}{10}\right)\frac{\partial^3 w_\varsigma}{\partial x^3}\right\}, \tag{45f}$$

$$\Lambda_{yyy} = -\frac{E_1 h}{2\,(1+\vartheta_{12})}\left\{\left(\frac{l_0^2}{6}+\frac{l_1^2}{15}\right)\frac{\partial^3 w_\varsigma}{\partial y^3}+\left(\frac{l_0^2}{6}-\frac{l_1^2}{10}\right)\frac{\partial^3 w_\varsigma}{\partial x^2 \partial y}\right\}. \tag{45g}$$

## References


1. McFarland, A.W., Colton, J.S.: Role of material microstructure in plate stiffness with relevance to microcantilever sensors. J. Micromech. Microeng. **15**, 1060–1067 (2005)
2. Poole, W.J., Ashby, M.F., Fleck, N.A.: Micro-hardness of annealed and work-hardened copper polycrystals. Scr. Mater. **34**, 559–564 (1996)
3. Stölken, J.S., Evans, A.G.: A microbend test method for measuring the plasticity length scale. Acta Mater. **46**, 5109–5115 (1998)
4. Koiter, W.T.: Couple stresses in the theory of elasticity, I and II. In: Proceedings of the Koninklijke Nederlandse Akademie van Wetenschappen. Series B: Physical Sciences, vol. 67, pp. 17–44 (1964)
5. Mindlin, R.D., Tiersten, H.F.: Effects of couple-stresses in linear elasticity. Arch. Ration. Mech. Anal. **11**, 415–448 (1962)
6. Toupin, R.A.: Theories of elasticity with couple-stress. Arch. Ration. Mech. Anal. **17**, 85–112 (1964)
7. Aifantis, E.C.: Gradient Deformation Models at Nano, Micro, and Macro Scales. J. Eng. Mater. Technol. **121**, 189–202 (1999)
8. Fleck, N.A., Hutchinson, J.W.: A phenomenological theory for strain gradient effects in plasticity. J. Mech. Phys. Solids **41**, 1825–1857 (1993)
9. Eringen, A.C.: Nonlocal polar elastic continua. Int. J. Eng. Sci. **10**, 1–16 (1972)
10. Eringen, A.C.: On differential equations of nonlocal elasticity and solutions of screw dislocation and surface waves. J. Appl. Phys. **54**, 4703–4710 (1983)
11. Eringen, A.C.: Theory of micropolar plates. Zeitschrift für Angew. Math. und Phys. ZAMP. **18**, 12–30 (1967)
12. He, X.Q., Kitipornchai, S., Liew, K.M.: Resonance analysis of multi-layered graphene sheets used as nanoscale resonators. Nanotechnology **16**, 2086–2091 (2005)
13. Kitipornchai, S., He, X.Q., Liew, K.M.: Continuum model for the vibration of multilayered graphene sheets. Phys. Rev. B. **72**, 075443 (2005)
14. Hosseini, M., Jamalpoor, A.: Analytical solution for thermomechanical vibration of double-viscoelastic nanoplate-systems made of functionally graded materials. J. Therm. Stress **38**, 1428–1456 (2015)
15. Murmu, T., Pradhan, S.C.: Buckling of biaxially compressed orthotropic plates at small scales. Mech. Res. Commun. **36**, 933–938 (2009)
16. Pradhan, S.C., Murmu, T.: Small scale effect on the buckling of single-layered graphene sheets under biaxial compression via nonlocal continuum mechanics. Comput. Mater. Sci. **47**, 268–274 (2009)
17. Duan, W.H., Wang, C.M.: Exact solutions for axisymmetric bending of micro/nanoscale circular plates based on nonlocal plate theory. Nanotechnology **18**, 385704 (2007)
18. Lam, D.C.C., Yang, F., Chong, A.C.M., Wang, J., Tong, P.: Experiments and theory in strain gradient elasticity. J. Mech. Phys. Solids **51**, 1477–1508 (2003)
19. Kong, S., Zhou, S., Nie, Z., Wang, K.: Static and dynamic analysis of micro beams based on strain gradient elasticity theory. Int. J. Eng. Sci. **47**, 487–498 (2009)
20. Akgöz, B., Civalek, Ö.: Analysis of micro-sized beams for various boundary conditions based on the strain gradient elasticity theory. Arch. Appl. Mech. **82**, 423–443 (2011)
21. Asghari, M., Kahrobaiyan, M.H., Nikfar, M., Ahmadian, M.T.: A size-dependent nonlinear Timoshenko microbeam model based on the strain gradient theory. Acta Mech. **223**, 1233–1249 (2012)
22. Ansari, R., Gholami, R., Sahmani, S.: Free vibration analysis of size-dependent functionally graded microbeams based on the strain gradient Timoshenko beam theory. Compos. Struct. **94**, 221–228 (2011)
23. Ashoori Movassagh, A., Mahmoodi, M.J.: A micro-scale modeling of Kirchhoff plate based on modified strain-gradient elasticity theory. Eur. J. Mech. A Solids **40**, 50–59 (2013)
24. Jamalpoor, a., Hosseini, M.: Biaxial buckling analysis of double-orthotropic microplate-systems including in-plane magnetic field based on strain gradient theory. Compos. B Eng. **75**, 53–64 (2015)
25. Yang, F., Chong, A.C.M., Lam, D.C.C., Tong, P.: Couple stress based strain gradient theory for elasticity. Int. J. Solids Struct. **39**, 2731–2743 (2002)
26. Park, S.K., Gao, X.-L.: Bernoulli–Euler beam model based on a modified couple stress theory. J. Micromech. Microeng. **16**, 2355–2359 (2006)

27. Tsiatas, G.C., Yiotis, A.J.: Size effect on the static, dynamic and buckling analysis of orthotropic Kirchhoff-type skew microplates based on a modified couple stress theory: comparison with the nonlocal elasticity theory. Acta Mech. **226**, 1267–1281 (2014)
28. Şimşek, M., Aydın, M., Yurtcu, H.H., Reddy, J.N.: Size-dependent vibration of a microplate under the action of a moving load based on the modified couple stress theory. Acta Mech. **226**, 3807–3822 (2015)
29. MA, H., GAO, X., REDDY, J.: A microstructure-dependent Timoshenko beam model based on a modified couple stress theory. J. Mech. Phys. Solids **56**, 3379–3391 (2008)
30. Fu, Y., Zhang, J.: Modeling and analysis of microtubules based on a modified couple stress theory. Phys. E Low Dimens Syst. Nanostruct. **42**, 1741–1745 (2010)
31. Ke, L.-L., Wang, Y.-S.: Flow-induced vibration and instability of embedded double-walled carbon nanotubes based on a modified couple stress theory. Phys. E Low Dimens. Syst. Nanostruct. **43**, 1031–1039 (2011)
32. Yin, L., Qian, Q., Wang, L., Xia, W.: Vibration analysis of microscale plates based on modified couple stress theory. Acta Mech. Solida Sin. **23**, 386–393 (2010)
33. Ma, H.M., Gao, X.-L., Reddy, J.N.: A non-classical Mindlin plate model based on a modified couple stress theory. Acta Mech. **220**, 217–235 (2011)
34. Ke, L.-L., Wang, Y.-S., Yang, J., Kitipornchai, S.: Free vibration of size-dependent Mindlin microplates based on the modified couple stress theory. J. Sound Vib. **331**, 94–106 (2012)
35. Lou, J., He, L.: Closed-form solutions for nonlinear bending and free vibration of functionally graded microplates based on the modified couple stress theory. Compos. Struct. **131**, 810–820 (2015)
36. Papargyri-Beskou, S., Beskos, D.E.: Static, stability and dynamic analysis of gradient elastic flexural Kirchhoff plates. Arch. Appl. Mech. **78**, 625–635 (2007)
37. Lazopoulos, K.A.: On bending of strain gradient elastic micro-plates. Mech. Res. Commun. **36**, 777–783 (2009)
38. Murmu, T., Sienz, J., Adhikari, S., Arnold, C.: Nonlocal buckling of double-nanoplate-systems under biaxial compression. Compos. B Eng. **44**, 84–94 (2013)
39. Raskovic, D.: Small forced damping vibrations of homogeneous torsional system with special static constraints. Publ. l'Institut Mathématique [Elektronische Ressource]. **3**, 27–34 (1963)
40. Rašković, D.: Small forced damping vibrations of homogeneous torsional system with special static constraints. Publ. l'Institut Mathématique. **3**, 27–34 (1963)
41. Stojanović, V., Kozić, P., Janevski, G.: Exact closed-form solutions for the natural frequencies and stability of elastically connected multiple beam system using Timoshenko and high-order shear deformation theory. J. Sound Vib. **332**, 563–576 (2013)
42. Akgöz, B., Civalek, Ö.: A microstructure-dependent sinusoidal plate model based on the strain gradient elasticity theory. Acta Mech. **226**, 2277–2294 (2015)
43. Akgöz, B., Civalek, Ö.: Modeling and analysis of micro-sized plates resting on elastic medium using the modified couple stress theory. Meccanica **48**, 863–873 (2012)
44. Pouresmaeeli, S., Ghavanloo, E., Fazelzadeh, S.A.: Vibration analysis of viscoelastic orthotropic nanoplates resting on viscoelastic medium. Compos. Struct. **96**, 405–410 (2013)